Epitaxial Growth of β-SiC on Si by RTCVD with C_3H_8 and SiH_4

Andrew J. Steckl, *Senior Member, IEEE,* and J. P. Li, *Student Member, IEEE*

Abstract—**The structural properties of β-SiC thin films grown on (100) Si by rapid thermal chemical vapor deposition (RTCVD) are reported. SiC growth was achieved by the reaction of SiH_4 (5% in H_2) and C_3H_8 (5% in H_2) from 1100 to 1300°C. The SiC growth was preceded by the formation of a carbonization buffer layer at 1200 to 1340°C. SiC growth rate of 0.5 to 1 nm/s was obtained. The SiC films were evaluated by X-ray diffraction, ellipsometry, SEM, and TEM analysis. From a structural point of view, the optimum conditions for carbonization were obtained at a temperature of 1300°C with a temperature ramp-up rate of around 50°C/s, a C_3H_8 flow rate of 11 sccm accompanied by 1.5 lpm H_2 flow. Optimum conditions for subsequent SiC growth were obtained at 1200°C, 11 sccm C_3H_8 flow rate, 13 sccm SiH_4 flow rate, and 1.5 lpm H_2 flow rate. Both X-ray and electron diffraction indicated a single-crystal expitaxial cubic SiC thin film. The 2θ peak at 41.44° characteristic of (100) SiC had a full width at half maximum (FWHM) signal of 0.18 to 0.22°. The propane flow rate has been observed to have a strong effect on the SiC film thickness, morphology, and void formation. A possible mechanism for this phenomenon has been proposed based on nucleation site density and Si surface diffusion.**

I. Introduction

Silicon carbide is currently receiving renewed interest [1] as an attractive candidate for semiconductor device applications involving "extreme" conditions: high temperature and/or radiation environments, high electrical power applications, high thermal power dissipation, etc. The relevance of SiC for these applications is a consequence of several of its properties: wide energy bandgap, high electron saturated drift velocity, high breakdown electric field, high thermal conductivity, good oxidation properties, imperviousness to most acids and other chemicals, etc.

The heteroepitaxial growth of SiC on Si substrate using conventional CVD reactors has yielded high-quality thin films with the 3C cubic crystal structure, commonly referred to as β-SiC. For example, Liaw and Davis [2] have reported on the epitaxial growth of β-SiC on both (100) and (111) Si using the reaction of silane (SiH_4) and ethylene (C_2H_4) at 1330°C. Nishino *et al.* [3] and Powell *et al.* [4] have reported similar SiC epitaxial growth using SiH_4 and propane (C_3H_8) at a growth temperature of 1360°C. In all cases the growth process was preceded by the carbonization of the Si surface obtained by the sole injection of the carbon gas precursor at a temperature close to that of the subsequent growth cycle. This chemical conversion of the surface to SiC has been shown by Nishino *et al.* [5], Addamiano and Klein [6], and others to be critical for the subsequent growth of epitaxial SiC. The carbonization process is generally anisothermal with the substrate experiencing a temperature ramp-up under C gas precursor flow. A relatively fast temperature ramp-up rate, ranging from ~10 to 50°C/s, has been reported [2], [3] by many authors to be necessary for the monocrystalline growth of subsequent SiC layers.

In the reports cited the growth process takes place in either a horizontal reactor (i.e., "diffusion" tube type) or in a vertical reactor ("barrel" type), with the substrate placed on a SiC-coated graphite susceptor heated by induction from an RF coil. While this inherently is a cold-wall process and has several advantages over the hot-wall deposition systems previously employed to grow SiC, it still has had to contend with the problems associated with a large susceptor: gas depletion effects, contamination effects, carbon contribution from the susceptor, etc. The susceptor used in SiC growth has been shown [7] to affect not only the structure and morphology of the SiC thin films but also their electrical properties.

In this paper we report on the heteroepitaxial growth of SiC-on-Si thin films by the rapid thermal chemical vapor deposition (RTCVD) technique. The RTCVD technique, also known as limited reaction processing [8], uses continuous gas flow of appropriate precursors in conjunction with the rapid heating and cooling capability of low thermal mass rapid thermal processing (RTP) equipment to control the growth process. Growth takes place only during the limited period the system is at high temperature. Gas switching occurs during the low-temperature segment of the process thus removing the transient effect of gas residence times. Therefore, RTCVD has the potential ability for growth of structures with very abrupt interfaces between thin films of various materials. Furthermore, the growth temperature, as well as other growth conditions, can be optimized separately for each material. This combination of characteristics makes RTCVD an interesting alternative to conventional CVD for the growth of heterostructures and for *in situ* processing. RTCVD has been successfully employed to grow Si [8] and GaAs [9] thin

Manuscript received November 8, 1990; revised August 20, 1991. This work was sponsored by the Ohio Edison Materials Technology Center.

The authors are with the Nanoelectronics Laboratory, University of Cincinnati, Cincinnati, OH 45221-0030.

IEEE Log Number 9103989.

0018-9383/92$03.00 © 1992 IEEE

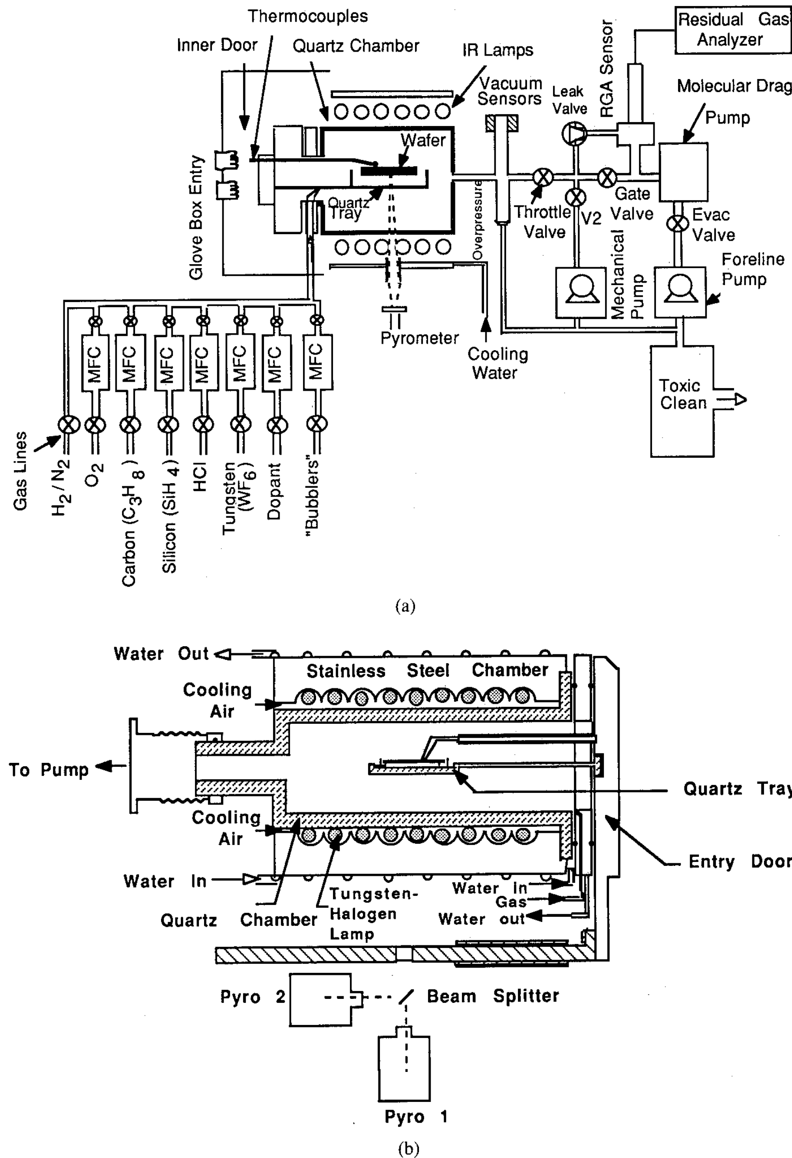

Fig. 1. Schematic diagram of (a) the RTCVD system and (b) the RTCVD reaction chamber.

films. For example, a multilayer p^+/p^- Si structure with a doping ratio of $>10^4$ and a period of ~ 230 nm has been fabricated [8] by RTCVD using $SiCl_2H_2$ at 850–950°C. This indicates that autodoping effects in Si epitaxial growth have been minimized by using the RTCVD technique. It is, therefore, very likely that the RTCVD growth of SiC will have a number of potential advantages over conventional CVD growth: a) ability to grow very thin films; b) ability to grow multiple layers *in situ*, such as needed for SiC–Si superlattice structures or for integrating several steps in the fabrication of a SiC transistor (e.g., growth, oxidation, metal deposition, etc.); c) ability to grow films at higher temperatures while still maintaining an overall restricted thermal budget; d) ability to tailor the carbonization ramp-up rate over a much wider range than in a conventional reactor; and e) elimination of contamination from the conventional susceptor.

II. Experimental Procedure and Conditions

The RTCVD system used in this study is a modified AET Addax RM unit. It consists of three main parts: the RTP reaction chamber, the pumping group, and a gas distribution system, as shown in Fig. 1(a). The reaction chamber (Fig. 1(b)) is fabricated from high-quality quartz. It has an oval cross section which enables both vacuum operation and large-area deposition (up to 10-cm diameter substrate) while efficiently utilizing the infrared output of

lamps placed on both sides of the chamber. The Si substrate is placed on three quartz pins of a quartz tray which is attached to a water-cooled door. The carbon contamination problem due to the graphite susceptor commonly used in the conventional CVD growth is thus completely eliminated. Two rows of nine high-power (6-kW) tungsten halogen lamps are used to heat the wafer. The lamps are enclosed within a stainless-steel chamber which has a reflective coating on the inner wall and is water-cooled. The wafer temperature is monitored by thermocouples and/or pyrometers.

The pumping system consists of a molecular drag pump in series with a mechanical pump, throttle valve, gate valve, foreline evacuation valve, V2, and overpressure valve. A thermocouple vacuum gauge and a cold-cathode vacuum gauge are used to indicate the chamber pressure. At the outlet of the mechanical pump a toxic gas cleaning system was installed to filter out the toxic residual precursors and by-products. The chamber base pressure achievable is about 1-2 $\times$ 10^{-6} torr.

There are seven process gas lines in the RTP system which are all equipped with pneumatically operated bellows seal valves and electronic mass flow controllers. The gases are introduced into the chamber through nozzles on the front door flange.

The operation of the RTP system is computer-controlled from an IBM-compatible PC. Simultaneous temperature, gas flow, and pressure versus time profiles are defined in a recipe file. The recipe can be executed under four processing modes: atmospheric processing, vacuum before and/or after atmospheric processing, vacuum processing, and user gas handling mode. In the user gas handling mode, the status and time duration of all the components in the vacuum system before and after the recipe execution are defined by the user. During recipe execution, the desired temperature and time recipe is obtained by a closed loop, real-time temperature control system which regulates the lamp power every 0.2 s by comparing the signal from the pyrometer (or thermocouple) with the existing temperature.

Normally, thermocouples react with certain processing gases at high temperature and thus can act as a contamination source. Therefore, only pyrometers which had been calibrated against the thermocouples are used during growth. The calibration accuracy of the pyrometer is within ± 3°C.

Ultra-high-purity hydrogen with less than 10 ppm total impurity content was used as the carrier gas. The gas sources of silicon and carbon were ultra-high-purity silane (diluted to 5% in H_2) with less than 5 ppm impurity content and propane (diluted to 5% in H_2) with less than 10 ppm impurity content. The flow rates of silane (or propane) referred to later in this paper indicate the rate of flow of the combined gas and its hydrogen diluent.

The substrates in most cases were standard (100) n-type Si wafers with 4-6-$\Omega \cdot$ cm resistivity. All samples were HF dipped and DI water rinsed just prior to being loaded into the chamber. The chamber was purged with high-purity nitrogen for about 5 min. It was then pumped down to about 5 $\times$ 10^{-4} torr. A typical procedure for carbonization was as follows:

a) H_2 flush for 2 min after pump-down;
b) HCl *in situ* cleaning: etching for 2 min at 1150°C with 45 sccm HCl in 3 lpm H_2;
c) pump-down to 5 $\times$ 10^{-4} torr;
d) introduction of process gases at programmed flow rates until atmospheric pressure is reached;
e) ramp-up to carbonization temperature at atmospheric pressure in the presence of 11 sccm C_3H_8 and 1.5 lpm H_2 with a ramp up rate of 50°C/s;
f) carbonization at 1300°C for 120-150 s.

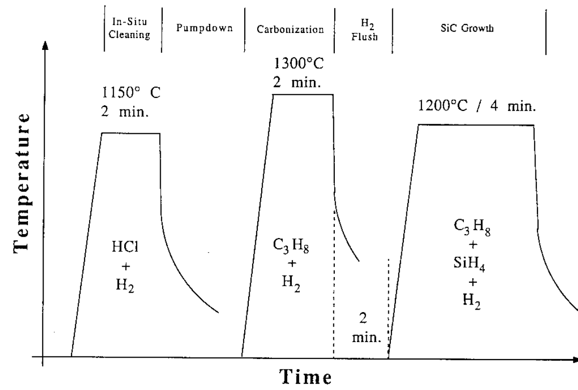

Fig. 2. SiC growth process diagram.

A typical growth procedure contained, in addition to the above carbonization procedure for 120 s, the following steps:

g) 2-min H_2 flush after termination of carbonization step;
h) ramp-up to growth temperature at 50°C/s in the presence of 13 sccm SiH_4, 11 sccm C_3H_8, and 1.5 lpm H_2; these flow rates result in a Si/C ratio in the gas phase of 0.43;
i) growth at 1200°C for 4 min.

The combined SiC growth process is shown schematically in Fig. 2. The gas-flow velocity in the reactor during either carbonization or growth was approximately 1 cm/s for 1.5 lpm H_2 flow.

III. Experimental Results and Discussion

The morphology of SiC films grown under the standard conditions listed in Section II is shown in Fig. 3 using phase contrast (Nomarski) optical microscopy. At low magnification, Fig. 3(a), the SiC films appear fairly smooth, and uniform. The surface roughness was evaluated by profilometer using a Dektak IIA system. SiC films obtained by carbonization for 90 to 150 s exhibit an *Ra* of 6 to 12 nm, whereas the virgin Si surface yielded a roughness of 3 nm. Post-carbonization growth for 4 min at 1200°C and 1300°C resulted in an *Ra* of 20 to 30 nm, respectively. Thus the surface roughness is approximately 5-10% of the film thickness. At higher magnification, Fig.

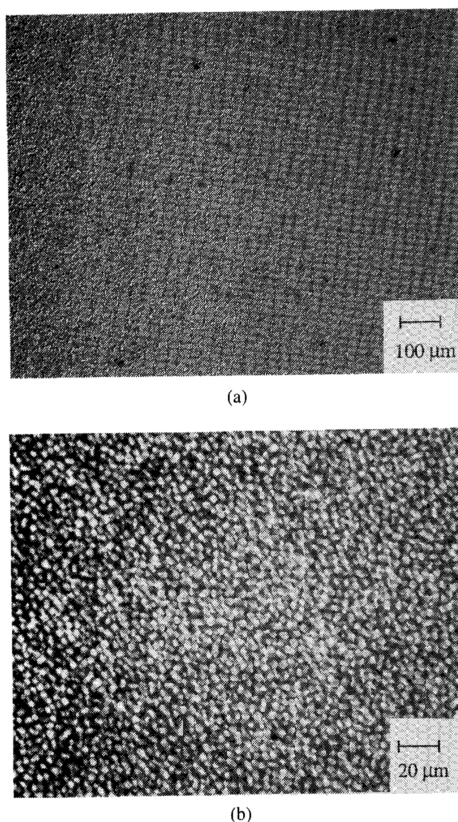

Fig. 3. Morphology of SiC for film obtained from carbonization (1300°C, 2 min) and growth (1200°C, 4 min) using optical microscopy. (a) Low magnification: 100×. (b) High magnification: 500×.

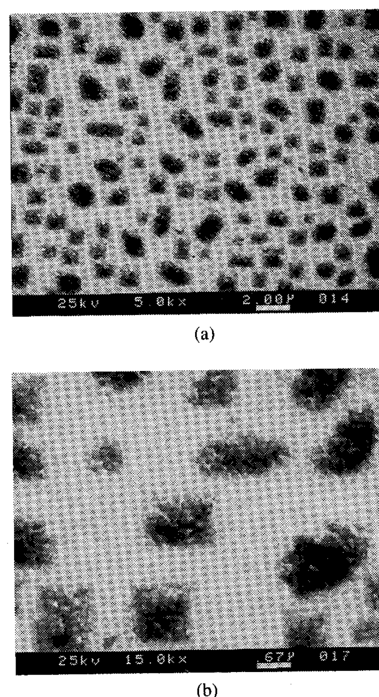

Fig. 4. Morphology of SiC film obtained from carbonization (1300°C, 2 min) and growth (1200°C, 4 min) using SEM. (a) Low magnification: 5k×. (b) High magnification: 15 k×.

3(b), a dense array of rectangular features is observed. These features are the bases of inverted rectangular pyramidal voids located in the Si subsurface region. Since SiC is transparent at optical wavelengths, these voids can be readily observed. The voids are reported to occur [2], [10] during carbonization as Si atoms diffuse through the converted layer to SiC nuclei on the growth surface where they react with C atoms and form additional SiC molecules. In the process Si vacancies consolidate in voids with edges parallel to the ⟨110⟩ directions and faces along the (111) planes in the Si substrate.

In plan-view SEM micrographs, the voids appear dark. As seen from Fig. 4(a) and (b) a typical dimension of the void base is of the order of 1 μm. Both square and rectangular voids are observed, with the long dimension of the rectangular void oriented at roughly 45° to the edges of the square voids. The void density is of the order of $10^7/\mathrm{cm}^2$. From Fig. 4(b) it can be seen that the SiC film extends over the voids.

Transmission electron microscopy was employed to investigate the morphology and crystallinity of the SiC thin films. Fig. 5(a) shows a plan-view TEM microphotograph of a film grown under the standard conditions described above. The film is continuous and fairly uniform, but exhibits a complex morphology consisting of swirls, loops, and small platelets. Transmission electron diffraction of the SiC film, shown in Fig. 5(b), displays a sharp single-crystal cubic structure. Calculation of the crystal lattice parameter from the Laue diffraction pattern yields a value of 4.4-Å which is quite close to the 4.359-Å value of bulk β-SiC. A cross-sectional TEM microphotograph of the same film is shown in Fig. 6. The SiC/Si interface is observed to be quite sharp and intimate. Twins, originating at the interface, are observed to extend into the film. The film thickness of 130-nm was quite uniform over the length of the film observed during TEM microscopy. The insert in Fig. 6 shows the transmission electron diffraction (TED) pattern obtained with the electron beam incident on the SiC–Si interface. The diffraction pattern exhibits both the SiC and Si (100) crystal structures in alignment with each other. The measured distances between spots for SiC and Si are in the ratio of 1.245, which is in excellent agreement with the inverse ratio calculated from the respective lattice constants, 1.246.

Extensive use was made of X-ray diffraction to determine the effect of various growth parameters. A Siemens diffractometer with a Cu source and with a system resolution of 0.08°, as determined from the full width at half-maximum of the (400) peak of a Si wafer, was used. Fig. 7(a) shows a full range X-ray spectrum of a bare Si (100) wafer. Both major (400) Si diffraction peaks, from Cu $K_{\alpha 1}$ and Cu $K_{\alpha 2}$ radiation, are observed at $2\theta = 69.1°$ and 69.3°, respectively. A small but sharp peak at 61.64° is associated with Cu K_β radiation. Fig. 7(b) shows the X-ray

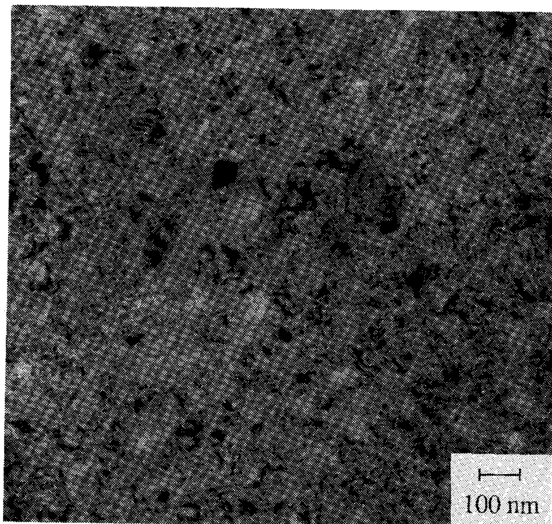

(a)

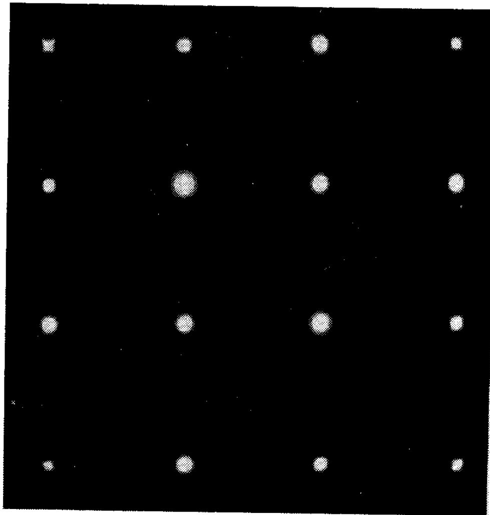

(b)

Fig. 5. TEM microphotographs of SiC film obtained from carbonization (1300°C, 2 min) and growth (1200°C, 4 min). (a) Plain view TEM—morphology and structure. (b) TEM diffraction pattern.

diffraction spectrum obtained from a Si wafer subjected to the carbonization process only (for 2 min at 1300°C in propane), while Fig. 7(c) contains the X-ray spectrum from a sample exposed to the entire SiC growth cycle (an additional 4 min at 1200°C in silane and propane). In addition to the Si peaks due to the substrate, two sharp peaks due to the cubic structure of the β-SiC are now apparent: $2\theta = 41.44°$ for the (200) reflection and 89.98° for the (400) reflection. The absence of any other SiC reflections indicate that the film is monocrystalline [11]. The measured FWHM of the SiC (200) peak of a fully processed SiC film is seen from Fig. 7(d) to be approximately 0.29°. This value is substantially smaller than the optimum values previously reported [3] for carbonization on (100) Si.

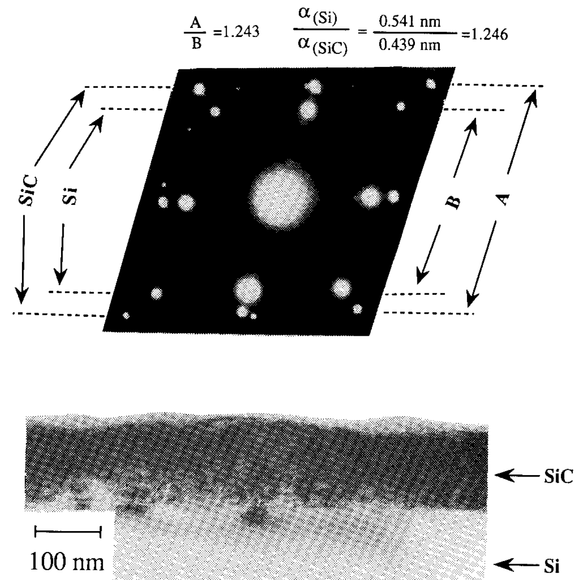

Fig. 6. Cross-sectional TEM microphotograph of SiC sample obtained by carbonization (1300°C, 2 min) and growth (1200°C, 4 min).

If the instrument resolution of 0.08° and the broadening effect due to the combination of $K_{\alpha 1}$ and $K_{\alpha 2}$ radiation dffraction of 0.1° are subtracted from the measured value, an even lower FWHM of 0.11° is obtained.

The level of the main SiC diffraction peak at 41.44° has been used as an indication of the structural quality of grown films. The SiC X-ray signal obtained under different growth conditions is shown normalized by the corresponding film thickness in order to compensate for volumetric effects. To check for system stability and measurement reproducibility, the X-ray diffraction signal from the Si substrate at 69.15° was periodically measured. A variation of approximately plus or minus 5% was observed. In conjunction with the X-ray signal, we have utilized the Laue pattern from TED to obtain a more consistent view of the SiC film quality as shown schematically at the top of each figure. To measure the thickness of the SiC films we first used cross-sectional SEM to determine an approximate value and thus determine the order for accurate ellipsometry measurements. Ellipsometry was performed with a Gaertner ellipsometer at 632.8 nm.

Let us first review the effect of the selected carbonization process parameters on the X-ray signal and thickness of the resulting films. In Fig. 8, the effect of reaction temperature is shown for films obtained with 7 sccm of C_3H_8 in 0.9 lpm of H_2 for 2.5 min. The film thickness increases monotonically with temperature, while the X-ray signal reaches a maximum for the film grown at 1300°C. A similar pattern in X-ray signal is also obtained for films grown for only 1.5 min, hence considerably thinner than their counterparts shown in Fig. 8 which were grown for 2.5 min. Therefore, the decrease in X-ray signal for films grown at 1340°C is not an effect due to the film exceeding

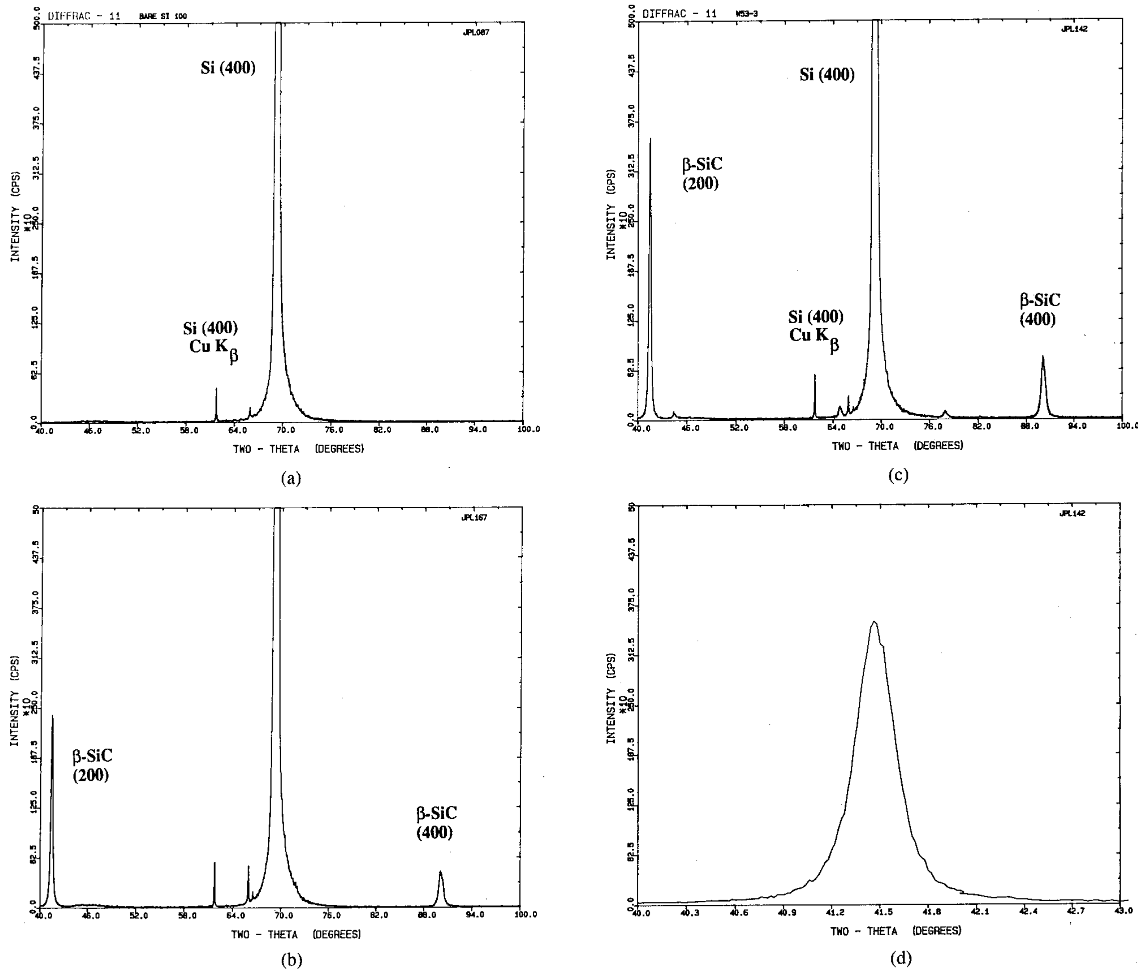

Fig. 7. X-ray diffraction spectra of Si and SiC. (a) Bare Si wafer. (b) Carbonization layer: 1300°C, 2 min. (c) Carbonization plus growth: 1200°C, 4 min. (d) SiC (200) peak from (c) on expanded scale.

a critical thickness, unless there is such a thickness for each temperature. This is a surprising result as one would normally expect at most a saturation in the X-ray signal with increasing temperature. Possible explanations include: a) differences in the relative arrival rates of C and Si atoms to the reacting surface; b) increase in the vertical growth rate relative to the horizontal (in-plane) growth rate.

The effect of ramp rate on the carbonization layer is shown in Fig. 9 for films grown at 1300°C for 2.5 min. It is interesting to note that while the ramp rate affects the growth rate only very slightly, it has a very strong effect on crystallinity. The optimum ramp rate appears to be around 25°C/s. While no single cause has been identified for the decrease in crystallinity at high ramp rate, a number of explanations are possible: a) desorption of SiO_2 and/or other surface contaminants does not occur fast enough prior to SiC growth initiation, leading to suboptimal nucleation; b) generation of fluid flow instabilities ("loops") because of the rapid thermal gradient experienced at high ramp rates, disturbing the nucleation process. A similar effect, namely, the degradation of SiC film crystallinity, has been reported [2], [4] when gases were rapidly introduced into chamber after the substrate reached high temperature.

The effect of propane flow on SiC film thickness is quite pronounced, with a critical range required for maximum film thickness. A representative example is shown in Fig. 10, where the 8- to 10-sccm flow rate represents the critical range. This characteristic behavior is always reproducible, with some variation in the actual values of optimum propane flow rates. While the X-ray signal appears to follow the same pattern, its interpretation is somewhat more complicated due to the inability of the diffractometer to accurately measure signals from very thin films. At higher propane flow rates the reduction in X-ray signal is accompanied by a decrease in film thickness, to the point where at 30 sccm little film growth is measured. The mechanisms responsible for the observed phenomenon are discussed below. We have used SEM to observe the sur-

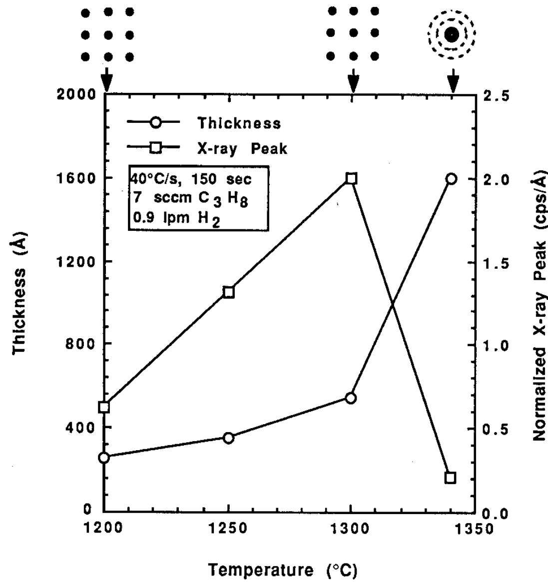

Fig. 8. SiC thickness and (200) X-ray peak versus temperature for carbonization process.

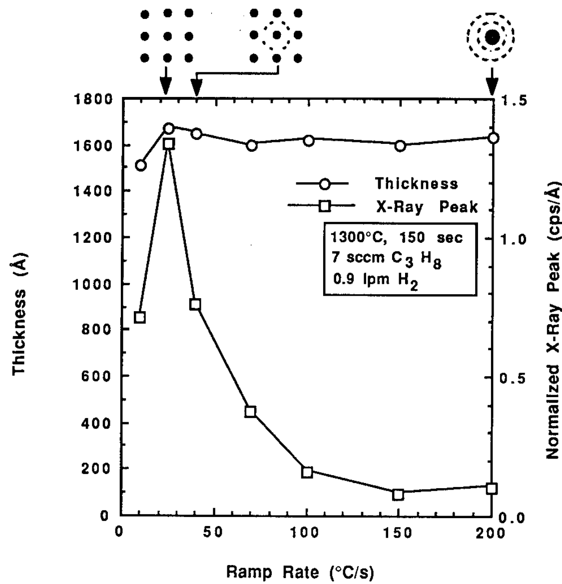

Fig. 9. SiC thickness and (200) X-ray peak versus ramp for carbonization process.

face morphology resulting at various propane flow rates at a constant reaction temperature (1300°C), time (90 s) and ramp rate (50°C/s). In the absence of propane, in other words hydrogen flow only, the Si surface after the same high-temperature cycle is smooth and featureless. Typical surface morphology obtained at low propane flow is shown in Fig. 11(a) and (b) for 2 and 4 sccm, respectively. For the 2-sccm case, small (<0.5 μm) isolated whitish particles are found after the reaction, with no evi-

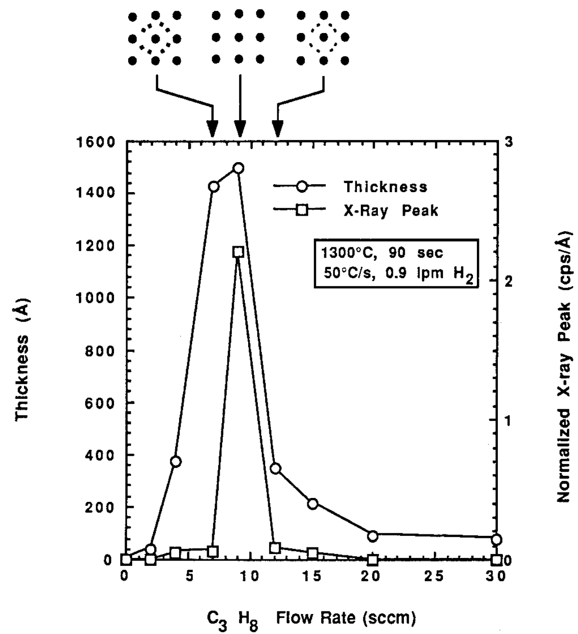

Fig. 10. SiC thickness and (200) X-ray peak versus propane flow for carbonization process.

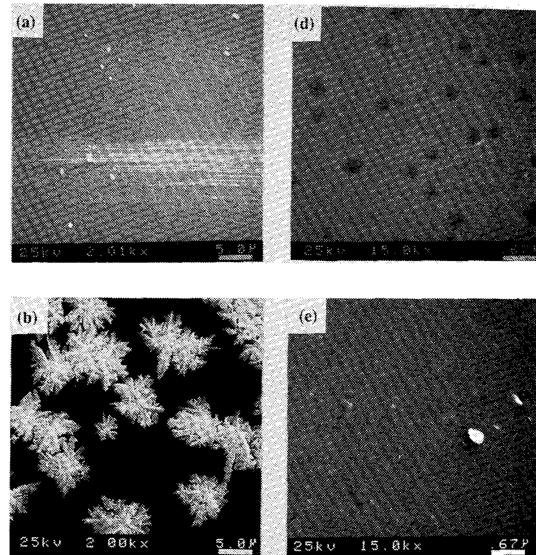

Fig. 11. SEM microphotographs of the surface after carbonization reaction at 1300°C for 1.5 min with 0.9 lpm H_2 and various propane flow rates. (a) 2 sccm. (b) 4 sccm. (c) 7 sccm. (d) 12 sccm. (e) 30 sccm.

dence of voids. At the propane flow rate of 4 sccm, significant snowflake-like deposits of 5–10 μm in size are formed over the entire surface. Extending the reaction time to 2.5 min resulted in the surface being mostly covered by overlapping snowflake structures. In neither case were the deposits removable by using a silicon etch ($HNO_3/HF/H_2O$). For propane flow rates from ~7 to ~11 sccm a high density of inverted pyramidal voids are observed. This is exemplified in Fig. 11(c) at 7 sccm. At propane flow rates higher than ~11 sccm, the void dimensions decrease while the frequency appears to increase, as shown in Fig. 11(d) for 12 sccm. Finally, for propane flow rate in excess of 20 sccm, only occasional voids are observed along with the reappearance of the isolated whitish deposits. This is illustrated in Fig. 11(e) at 30-sccm flow rate.

To investigate the time-dependent behavior of the pyramidal voids, we have studied the surface morphology obtained after a very rapid carbonization of nominally only 1 s at 1300°C with 7 sccm C_3H_8 and 0.9 lpm H_2. For such short reaction times the temperature ramp rate has a much stronger effect on the energy introduced into the reaction. In the case of a nominal reaction time of 1 s at 1300°C and ramp-up and ramp-down rates of 50°C/s and 130°C/s, respectively, the total effective exposure time is calculated to be approximately 2.5 s. This was calculated taking into account an Arrhenius-type reaction with an activation energy of 3.1 eV. As seen in Fig. 12(a), the void dimensions are much smaller (0.2–0.3 μm) than those seen in Fig. 11(c) for 90-s reaction time, while the void frequency is substantially increased. Occasional "giant" voids are also observed with dimensions of ~5–10 μm, as shown in Fig. 12(b). A closeup of a giant void is shown in Fig. 12(c). Agglomerations of smaller voids are seen along the intersections of the (111) planes. Cross-sectional TEM has been used to check the film continuity and measure its thickness after the 1-s growth period. Shown in Fig. 13(a) are xTEM microphotographs of the 1-s growth taken at different locations. An almost continuous SiC film of ~8 nm is observed covering the Si surface. In the upper photograph, cross-sections of two voids are observed, indicating that the void depth after 1-s growth reaches ~100–200 nm. It is instructive to compare the xTEM photographs (Fig. 13(a) obtained after 1 s at 1300°C in 7 sccm C_3H_8 with that obtained after 90 s at 1300°C in 30 sccm C_3H_8 (Fig. 13(b)). The two conditions result in approximately the same film thickness. However, the high propane flow rate film, which has a much lower growth rate, exhibits no voids.

To understand the effect of propane flow rate on growth rate and void formation we have measured the film thickness obtained for several reaction times and various flow rates. As shown in Fig. 14, the high propane flow rate (30 sccm) results in a saturation of the SiC film thickness (d_s) at a very low value. This saturation occurs within a very short time ($t_s \approx 10$ s) under the conditions used. The intermediate flow rate of 9 sccm results in a high initial growth rate and eventually saturates at $t_s \approx 90$ s. Finally,

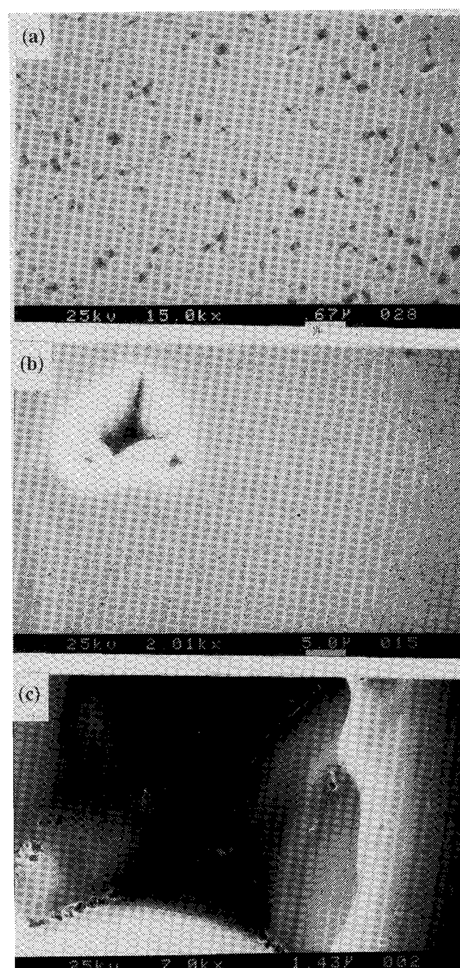

Fig. 12. SEM microphotographs of the surface after carbonization at 1300°C for 1 s with 7 sccm C_3H_8 and 0.9 lpm H_2. (a) Regular voids. (b) Giant void. (c) Closeup of giant void.

the low flow rate of 5 sccm yields a smaller initial growth rate than the 9 sccm case, but apparently saturates at a longer t_s and consequently thicker d_s.

One can reasonably explain a number of these observations on the basis of nucleation site density. Under high propane flow rate conditions, there are presumably numerous nucleation sites available, thus preventing the establishment of preferred Si outdiffusion locations and subsequent void formation. At the same time, the large number of nucleation sites result in a continuous film being rapidly grown. Once the Si surface is completely sealed, further carbonization requires the diffusion of either Si or C through the SiC film to the top surface or to the SiC–Si interface, respectively. The diffusivities for these processes is very low [15] and, hence, the growth essentially stops for films of thickness beyond a very small value. At low propane flow rates, there are relatively fewer nucleation sites, resulting in three-dimensional dendritic growth. Therefore, a considerable portion of the Si surface continues to be exposed for a long time, leading

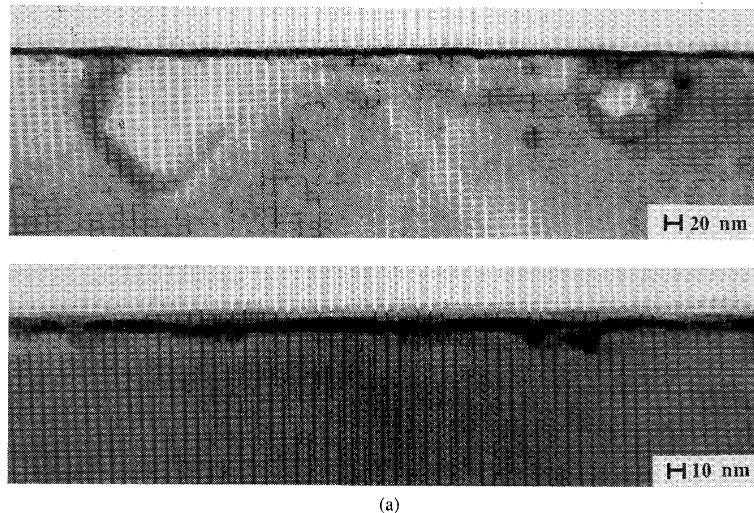

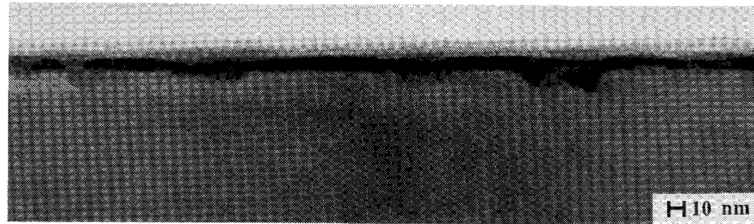

(a)

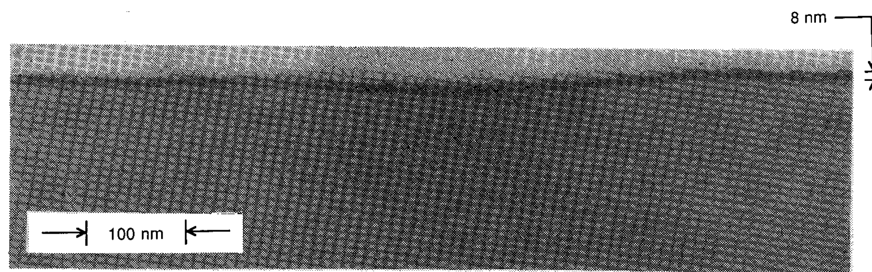

(b)

Fig. 13. Cross-sectional TEM microphotographs of SiC film after carbonization at 1300°C. (a) 1-s growth with 7 sccm C_3H_8. (b) 90-s growth with 30 sccm C_3H_8.

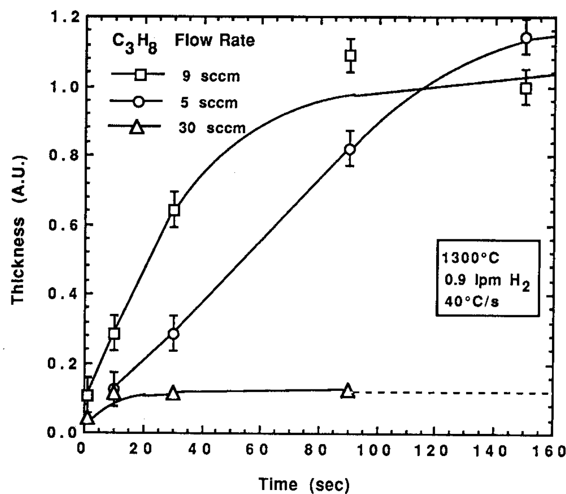

Fig. 14. SiC film thickness versus time at various C_3H_8 flow rates.

to a long saturation time and thickness. At intermediate flow rates, sufficient nucleation sites produce primarily two-dimensional growth. Vias in the film allow Si atoms to diffuse from void locations along the Si and then SiC surfaces to the reaction sites on the top surface. The initial growth rate at intermediate propane flow rate is higher than that for the low flow rate case since more nucleation sites are available. However, as the vias in the film become sealed the growth rate declines below that of the low flow-rate case.

The effect of increasing the hydrogen flow rate at a fixed propane flow, shown in Fig. 15, is equivalent to the dilution of the propane gas concentration. This results in a monotonically decreasing X-ray signal. Finally, the effect of hydrogen flow rate with a fixed C_3H_8/H_2 ratio of 7.5×10^{-3} is shown in Fig. 16. The optimum condition occurs for a 1.5 lpm H_2 flow rate.

Let us now turn to the thin film measurements of SiC post-carbonization growth. Preliminary experiments were performed using a fixed C_3H_8 flow rate (11 sccm) while varying the SiH_4 flow rate and the reaction temperature. The effect of growth temperature for Si/C ratio (in the gas) of 0.4 is shown in Fig. 17. The optimum temperature is $\sim 1200°C$, yielding a maximum in X-ray signal. The effect of changing the Si/C ratio (i.e., silane/propane flow rate ratio) is shown in Fig. 18. The results indicate that a Si/C ratio from 0.2 to 0.4 is preferable.

Electron energy loss spectroscopy (EELS) was also used to verify the SiC bonding structure at the film surface. Using a 10-eV primary electron beam, the energy

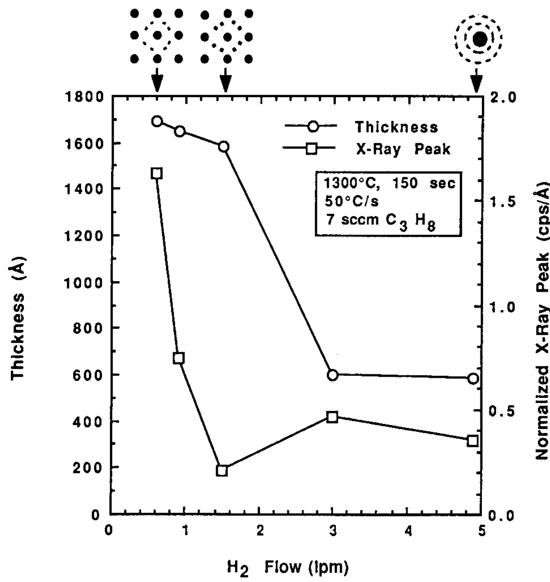

Fig. 15. SiC thickness and (200) X-ray peak versus H_2 flow for carbonization process with 7-sccm propane flow rate.

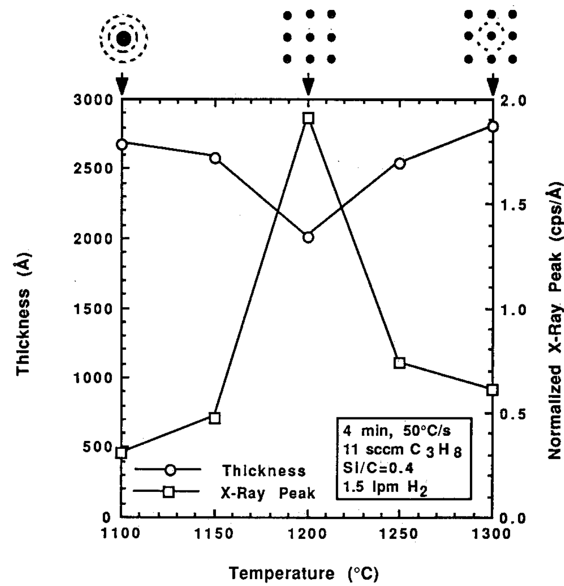

Fig. 17. SiC thickness and (200) X-ray peak versus temperature for post-carbonization growth with Si/C ratio of 0.4.

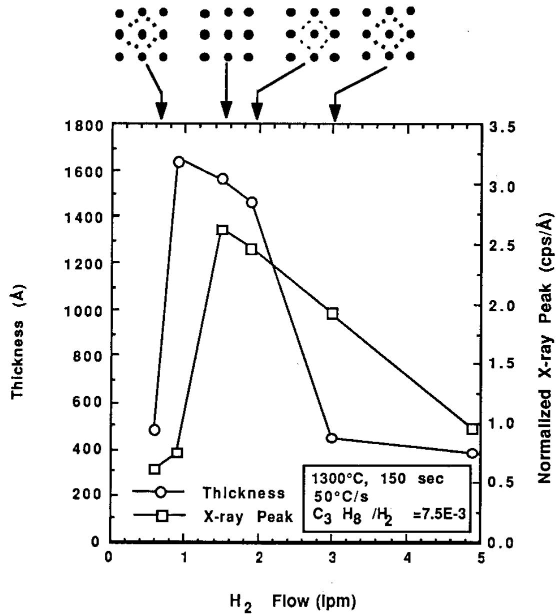

Fig. 16. SiC thickness and (200) X-ray peak versus flow of H_2 for carbonization process with constant propane/hydrogen flow rate ratio.

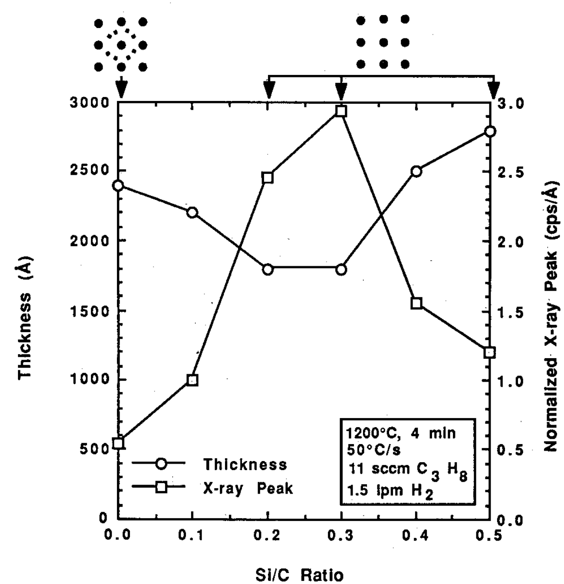

Fig. 18. SiC thickness and (200) X-ray peak versus Si/C ratio for post-carbonization growth at 1200°C.

loss spectrum shown in Fig. 19 was obtained from a sample carbonized at 1300°C for 3 min. The elastic peak (I_0) exhibited an FWHM of 27.4 meV, as compared to 13 meV for a bare Si sample. The Si–C bond resulted in a peak (I_1) at ~930 cm^{-1} (116 meV) with an FWHM of ~34.6 meV. The I_1/I_0 ratio has a value of ~0.27. The second-order loss peak is observed at 1860 cm^{-1}. No other peaks are observed, including the Si–Si, C–C, C–H. Previously reported [13], [14] EELS measurements on SiC-on-Si thick (5–15 μm) films grown by CVD generally were performed after high-temperature (1285°C) annealing. In that case the same Si–C loss peak at 116 meV was observed. This indicates that even for SiC films as thin as 100–200 nm the Si–C bonding is fully formed at the surface.

In summary, we have established that β-SiC thin films can be grown epitaxially on (100) Si substrates by RTCVD employing carbonization with C_3H_8, as well as post-carbonization growth using SiH_4 and C_3H_8 in H_2. In particular, we have determined the optimum carbonization con-

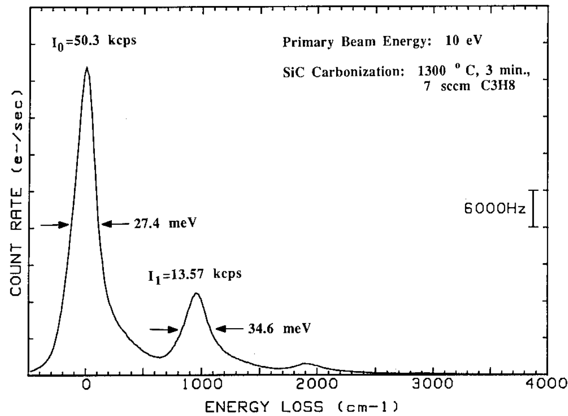

Fig. 19. EELS spectrum for SiC carbonization process at 1300°C, 2 min.

ditions with respect to reaction temperature and ramp rate, gas flow rates, etc. A possible mechanism, based on nucleation density and Si surface diffusion, has been proposed for the effect of C_3H_8 flow rate on film thickness, morphology, and void formation. Void-free SiC films have been grown on Si at high C_3H_8 flow rates. We have also determined the optimum conditions for subsequent SiC growth with respect to temperature and Si/C ratio in the gas phase. We have established that the resulting SiC thin films are monocrystalline by X-ray and electron diffraction. Using EELS we have observed only the Si–C bonding at the surface of the films. The SiC–Si interface was investigated by cross-section TEM and found to be sharp and intimate where no voids are present.

Acknowledgment

The assistance of S. Mogren, D. Irvin, and P. Moreton in the installation and operation of the RTCVD system is much appreciated. Assistance in the X-ray measurements was received from M. Phillips and useful discussions on X-ray diffraction were held with J. Grover. Similarly, the assistance in TEM analysis of A. K. Rai is gratefully acknowledged. Assistance in ellipsometry from G. DeBrabander and J. T. Boyd is also acknowledged. Finally, interesting discussions on surface properties and EELS measurements with A. T. Hubbard and J. Gui were much appreciated.

References

[1] J. A. Powell and L. G. Matus, "Recent developments in SiC," in *Amorphous and Crystalline Silicon Carbide* (Springer Proc. in Physics), vol. 34, G. L. Harris and C. Y.-W. Yang, Eds. New York: Springer-Verlag, 1989, pp. 2–12.

[2] P. Liaw and R. F. Davis, "Epitaxial growth and characterization of β-SiC thin films," *J. Electrochem. Soc.*, vol. 132, no. 3, pp. 642–648, Mar. 1985.

[3] S. Nishino, H. Suhara, H. Ono, and H. Matsunami, "Epitaxial growth and electric characteristics of cubic-SiC on silicon," *J. Appl. Phys.*, vol. 61, no. 10, pp. 4889–4893, May 15, 1987.

[4] J. A. Powell, L. G. Matus, and M. A. Kuczmarski, "Growth and characterization of cubic single-crystal SiC films on Si," *J. Electrochem. Soc.*, vol. 134, no. 6, pp. 1558–1565, June 1987.

[5] S. Nishino, J. A. Powell, and H. A. Will, "Production of large-area single-crystal wafers of cubic SiC for semiconductor devices," *Appl. Phys. Lett.*, vol. 42, no. 5, pp. 460–463, Mar. 1, 1983.

[6] A. Addamiano and P. H. Klein, "Chemically-formed buffer layers for growth of cubic silicon carbide on silicon single crystals," *J. Crystal Growth*, vol. 70, pp. 291–294, 1984.

[7] J. A. Powell and L. G. Matus, "Chemical vapor deposition of single crystal β-SiC," in *Amorphous and Crystalline Silicon Carbide II* (Springer Proc. in Physics), vol. 43, M. M. Rahman and C. Y. Yang, Eds. New York: Springer-Verlag, 1989, pp. 14–19.

[8] C. M. Gronet, J. C. Sturm, K. E. Williams, and J. F. Gibbons, "Thin, highly doped layers of epitaxial silicon deposited by limited reaction processing," *Appl. Phys. Lett.*, vol. 48, no. 15, Apr. 14, 1986.

[9] S. K. Reynolds, "Application of rapid thermal processing to epitaxy and doping of gallium arsenide," Ph.D. dissertation, Stanford University, Stanford, CA, 1987.

[10] T. T. Cheng, P. Pirouz, and J. A. Powell, "The buffer layer in the CVD growth of β-SiC on (001) silicon," *MRS Proc.*, vol. 148, pp. 229–234, 1989.

[11] B. C. Johnson, J. M. Meese, G. W. Zajac, J. O. Schreiner, J. A. Kaduk, and T. H. Fleisch, "Characterization and growth of SiC epilayers on Si substrates," *Superlattices and Microstructures*, vol. 2, no. 3, pp. 223–231, 1986.

[12] P. T. Shaffer and R. G. Naum, "Refractive index and dispersion of beta silicon carbide," *J. Opt. Soc. Amer.*, vol. 59, no. 1, p. 1498, Nov. 1970.

[13] M. Dayan, "High resolution EELS on the (100) surface of β-SiC," *Surface Sci. Lett.*, vol. 149, pp. L33–L38, 1985.

[14] M. Dayan, "The β-SiC (100) surface studied by low energy electron diffraction, Auger electron spectroscopy and electron energy loss spectra," *J. Vac. Sci. Technol.*, vol. A4, no. 1, pp. 38–45, Jan./Feb. 1986.

[15] C. J. Mogab and H. J. Leamy, "Epitaxial growth of β-SiC on Si: Kinetics and growth mechanisms," in *Silicon Carbide—1973*. Columbia, SC: Univ. of South Carolina Press, 1974.

*

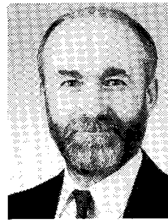

Andrew J. Steckl (S'70–M'73–SM'79) received the B.S.E. degree in electrical engineering from Princeton University, Princeton, NJ, in 1968, and the M.Sc. and Ph.D. degrees from the University of Rochester, Rochester, NY, in 1970 and 1973, respectively.

In 1972, he joined the Honeywell Radiation Center, Lexington, MA, as a Senior Research Engineer, where he worked on new concepts and devices in the area of infrared detection. In 1973, he joined the Technical Staff of the Electronics Research Divison of Rockwell International, Anaheim, CA. At Rockwell he was primarily involved in research on charge coupled devices. In 1976, he joined the Electrical, Computer and Systems Engineering Department at Rensselaer Polytechnic Institute in Troy, NY, where he developed a research program in microfabrication of Si devices. In 1981, he initiated the Center for Integrated Electronics, a multi-disciplinary academic center focused on VLSI research and teaching, and served as its director until 1986. In 1988, he joined the Electrical and Computer Engineering Department of the University of Cincinnati as Ohio Eminent Scholar and Gieringer Professor of Solid State Microelectronics. At Cincinnati he has built the Nanoelectronics Laboratory whose mission is to investigate materials, fabrication techniques, and devices operating at the nanometer level. His research interests include focused ion beam fabrication of Si and compound semiconductor devices, SiC thin-film growth and device fabrication, reactive ion etching, and atomic scale microscopy. His research has resulted in 125 publications and over 150 conference and seminar presentations.

*

J. P. Li (S'88) was born in PuQi, China, in 1963. He received the B.S. and M.S. in optical engineering from Tsinghua University, Beijing, China, in 1984 and 1987, respectively. He is currently a Ph.D. candidate in the Department of Electrical and Computer Engineering at the University of Cincinnati, Cincinnati, OH.

Since September 1987, he has been working with Prof. A. J. Steckl doing research on the heteroepitaxial nucleation and growth of SiC thin films, rapid thermal CVD, and fluid flow visualization.